Mechanistic Probes of Zinc Anode Aqueous Electrolyte Batteries

Esther S. Takeuchi, SUNY Distinguished Professor, Stony Brook University
William and Jane Knapp Chair in Energy and the Environment
Chair, Interdisciplinary Science Department, Brookhaven National Laboratory

Kenneth J. Takeuchi, SUNY Distinguished Teaching Professor, Stony Brook University

Amy C. Marschilok, Associate Professor, Stony Brook University
Manager, Energy Storage Division, Brookhaven National Laboratory

Outline

Background

Mechanistic Study

Summary

Acknowledgements

Background: Zn/α-MnO_2 Batteries

α-MnO_2 has been investigated as a cathode materials for Zn-ion batteries

Despite promising electrochemistry, the **underlying charge storage mechanism remains unclear**

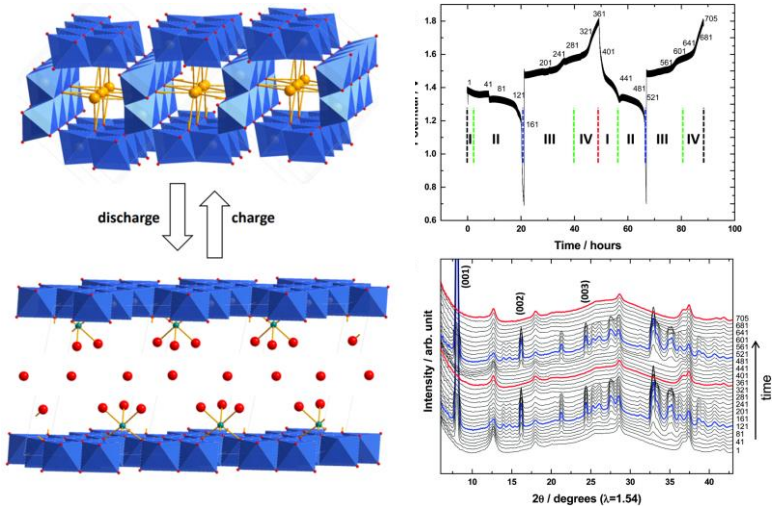

Zn-Insertion Reaction: Reversible formation of layered structure, $ZnMn_3O_7 \cdot 3H_2O$ with large inter-planar spacing upon discharge

Lee, B.; Lee, H. R.; Kim, H.; Chung, K. Y.; Cho, B. W.; Oh, S. H. *Chem. Commun.* **2015**, *51*, 9265-9268.

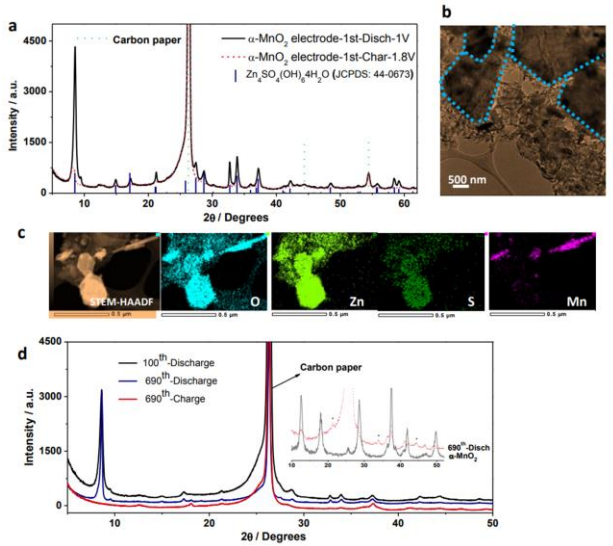

Chemical Conversion Reaction: Insertion of H^+ and formation of MnOOH and $Zn_4SO_4(OH)_6$. Return of α-MnO_2 and dissolution of $Zn_4SO_4(OH)_6$ on charge. No indication of Zn-insertion

Pan, H.; Shao, Y.; Yan, P.; Cheng, Y.; Han, K. S.; Nie, Z.; Wang, C.; Yang, J.; Li, X.; Bhattacharya, P., *et al.* . *Nat. Energy* **2016**, *1*, 16039.

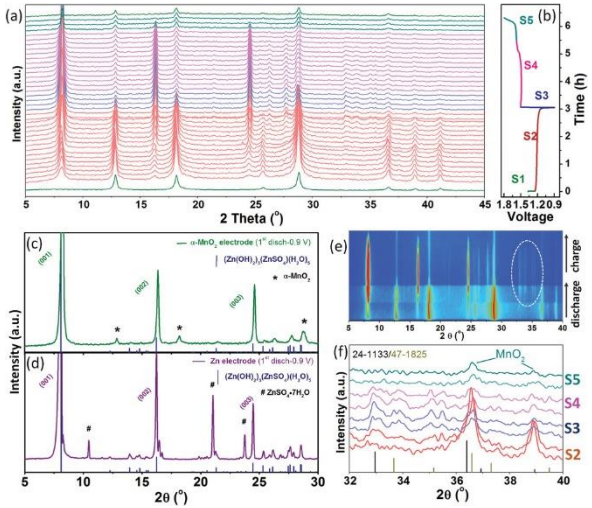

H^+ and Zn^{2+} Co-insertion/Conversion: Insertion of H^+ and Zn^{2+}. Reversible formation of $Zn_4SO_4(OH)_6$. Zn^{2+} intercalation forming spinel $ZnMn_2O_4$.

Gao, X.; Wu, H.; Li, W.; Tian, Y.; Zhang, Y.; Wu, H.; Yang, L.; Zou, G.; Hou, H.; Ji, X. *Small* **2020**, *16*, 1905842.

Zn/α-MnO_2 Electrochemistry and Crystallographic Structure After Cycling

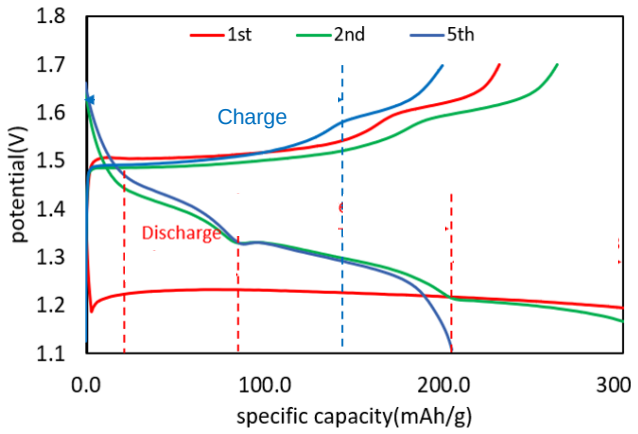

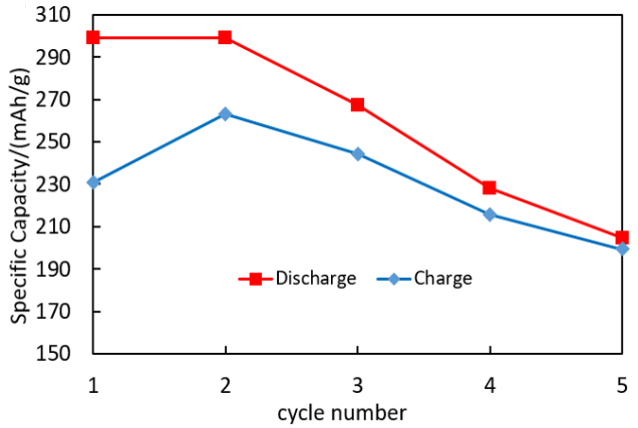

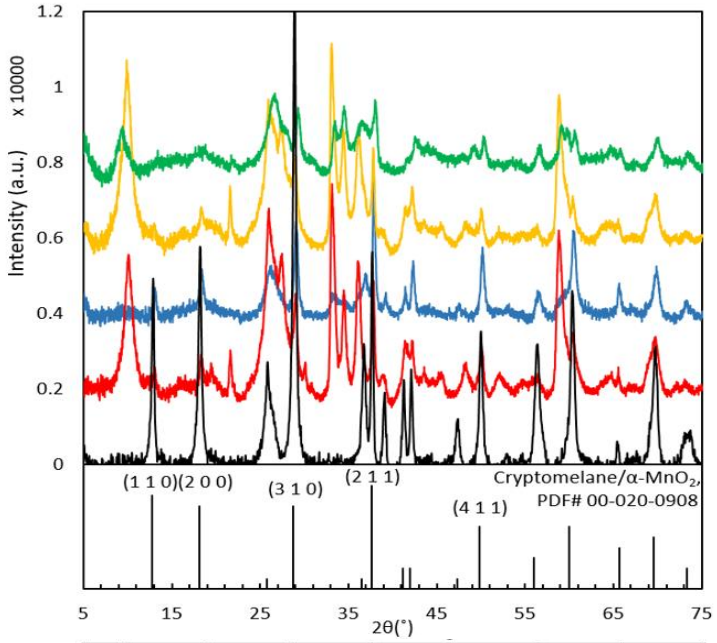

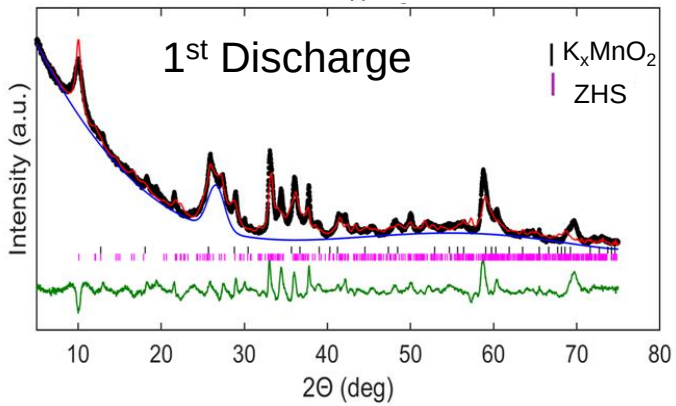

Phase composition of pristine and (dis)charge products determined by Rietveld Refinement.

Pristine - Kα-MnO_2 (100%)

Cycle 1 Discharge – Kα-MnO_2 (64%) and $Zn_4SO_4(OH)_6{\cdot}3H_2O$ (36%)

Cycle 1 Charge - Kα-MnO_2 (100%)

Cycle 5 Discharge - Kα-MnO_2 (42%) and $Zn_4SO_4(OH)_6{\cdot}5H_2O$ (58%)

Cycle 5 Charge – Broken-tunneled Kα-MnO_2 (78%) and Layered Chalcophanite Structure, $ZnMn_3O_7{\cdot}3H_2O$ (22%)

D. Wu, L.M. Housel, S-J. Kim, N. Sadique, C.D. Quilty, L. Wu, R. Tappero, S.L. Nicholas, S. Ehrlich, Y. Zhu, A.C. Marschilok, E.S. Takeuchi, D.C. Bock, K.J. Takeuchi, Energy & Environmental Science (2020). DOI: 10.1039/d0ee02168g.

Scanning Transmission Electron Microscopy (TEM) After Cycling

Cycle 1 Discharge

Cycle 1 Charge

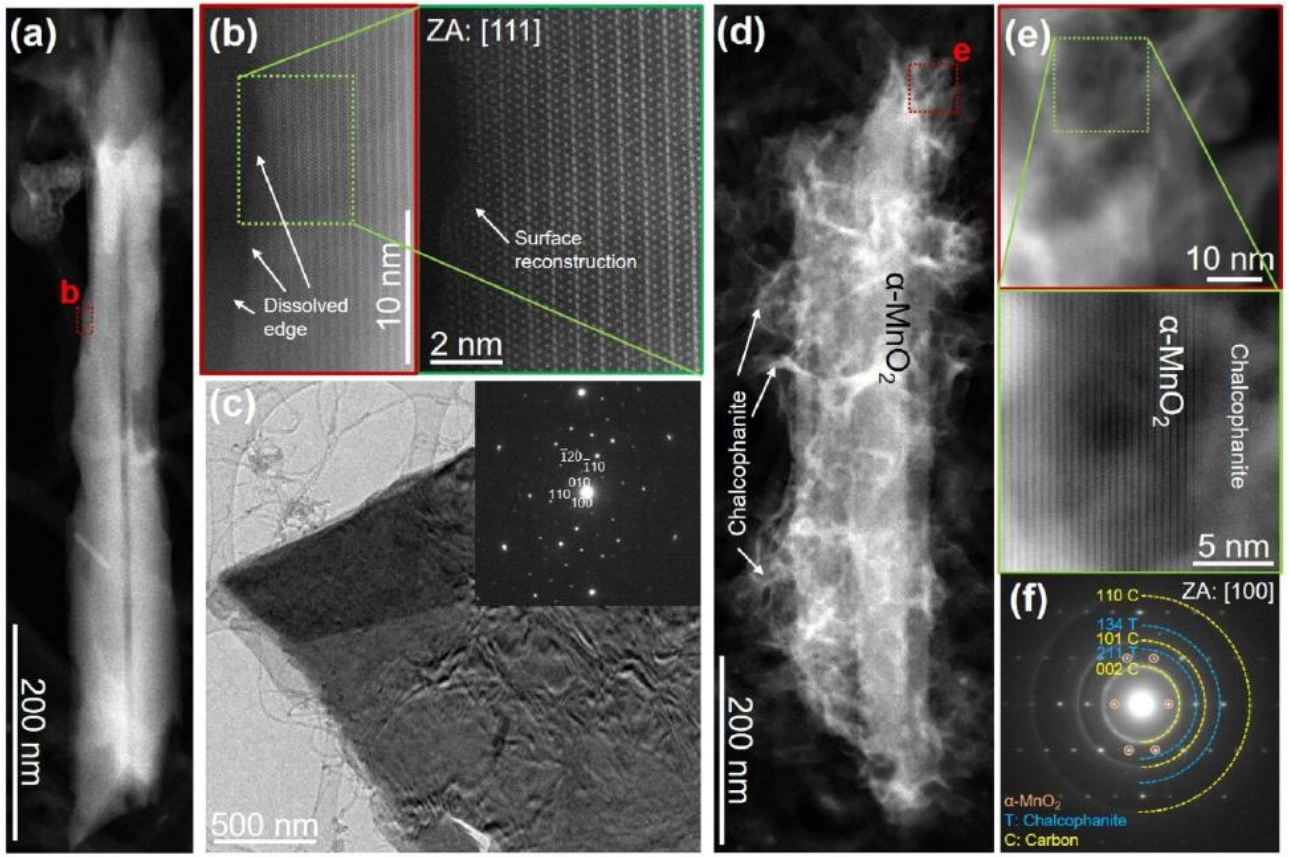

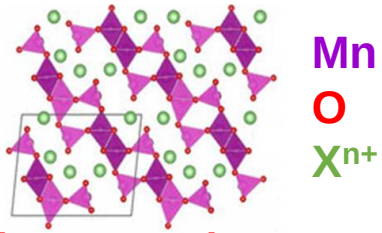

Broken Tunnel α-MnO_2

A.B. Brady, K.R. Tallman, E.S. Takeuchi, A.C Marschilok, K.J. Takeuchi, P. Liu, *The Journa Physical Chemistry C* **2019,** *123* (41), 25042-25051.

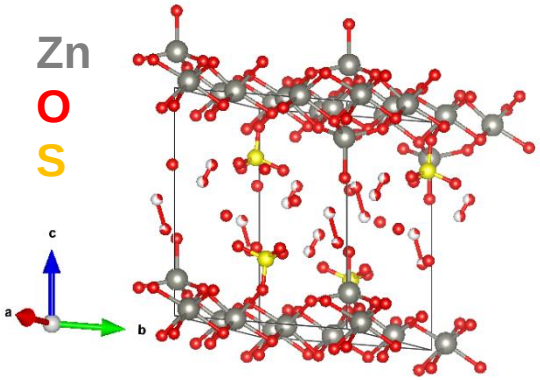

ZHS ($Zn_4SO_4(OH)_6{\cdot}5H_2O$)

PDF Card: 00-060-0655

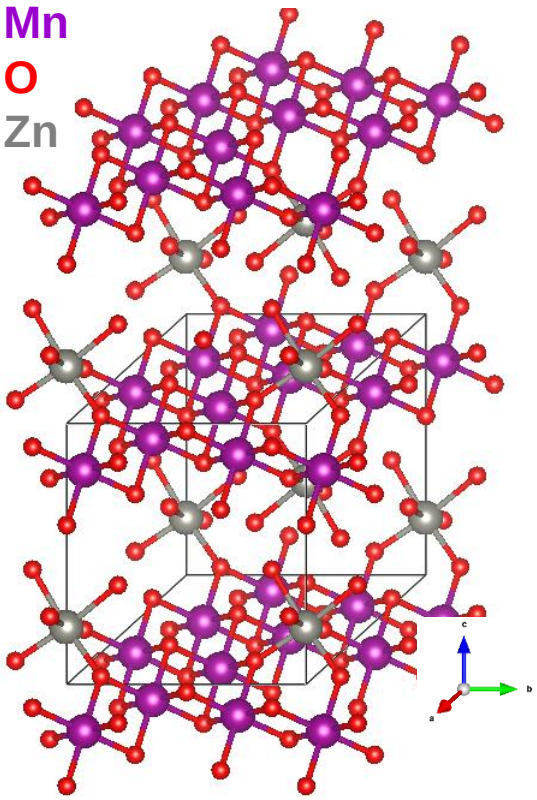

Chalcophanite ($ZnM_3O_7{\cdot}3H_2O$)

A.D. Wadsley, *Nature*, 1953, **172**, 1103-1104.

ZHS formation on discharge & cryptomelane/Chalcophanite co-existence upon charge

D. Wu, L.M. Housel, S-J. Kim, N. Sadique, C.D. Quilty, L. Wu, R. Tappero, S.L. Nicholas, S. Ehrlich, Y. Zhu, A.C. Marschilok, E.S. Takeuchi, D.C. Bock, K.J. Takeuchi, Energy & Environmental Science (2020). DOI: 10.1039/d0ee02168g.

Ex-situ XAS Determined Chemical and Local Atomic Structure

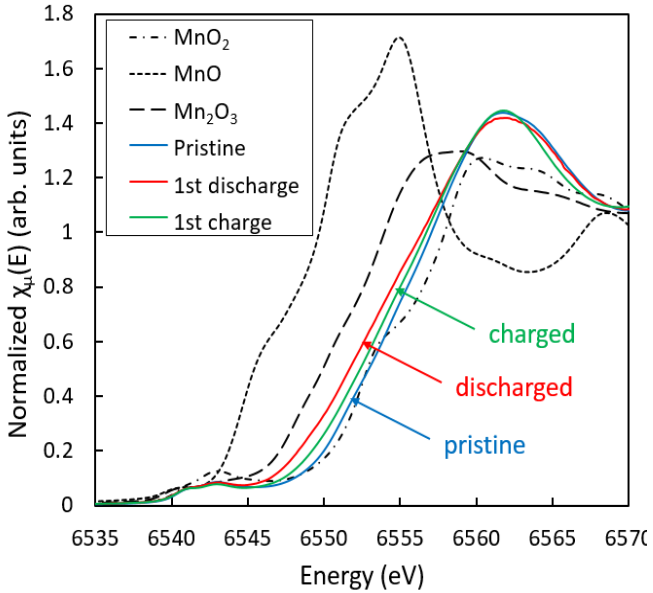

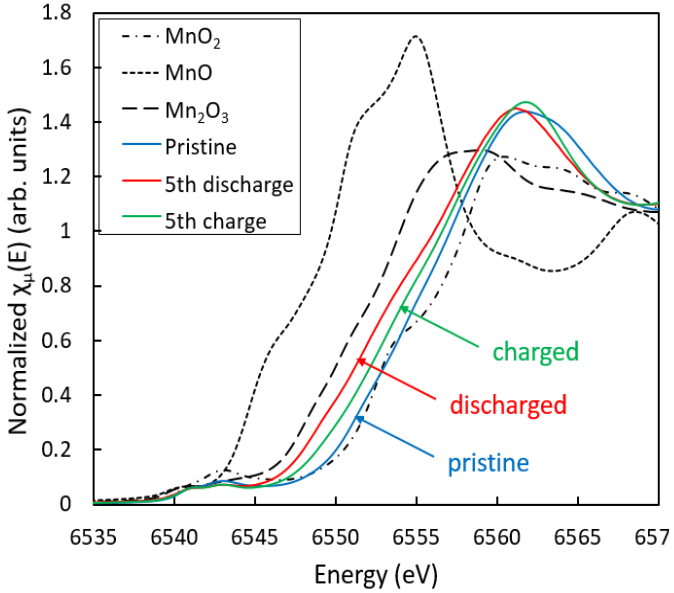

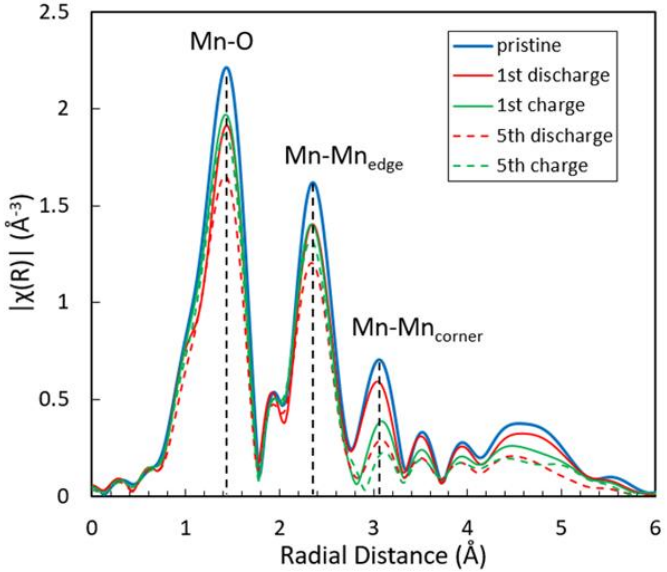

Sample	Mn^{n+} (LCF)	Expected specific capacity (LCF) (mAh/g)	Actual specific capacity (mAh/g)
Pristine	3.880	N/A	N/A
1st discharge	3.603	81	300
1st charge	3.741	40	227
5th discharge	3.468	N/A	211
5th charge	3.672	60	200

Mn^{n+} change between charge and discharge transfers does not fully account for delivered capacity

$Mn\text{-}Mn_{corner}$ interactions reduce over cycles, indicating breakage of tunnels

Cycle 5 charged sample fit to broken-tunnel α-MnO_2 and Chalcophanite, $ZnM_3O_7{\cdot}3H_2O$

D. Wu, L.M. Housel, S-J. Kim, N. Sadique, C.D. Quilty, L. Wu, R. Tappero, S.L. Nicholas, S. Ehrlich, Y. Zhu, A.C. Marschilok, E.S. Takeuchi, D.C. Bock, K.J. Takeuchi, Energy & Environmental Science (2020). DOI: 10.1039/d0ee02168g.

Quantifying Mn^{n+} via Spatio-Temporally Resolved X-ray Fluorescence (XRF) Mapping

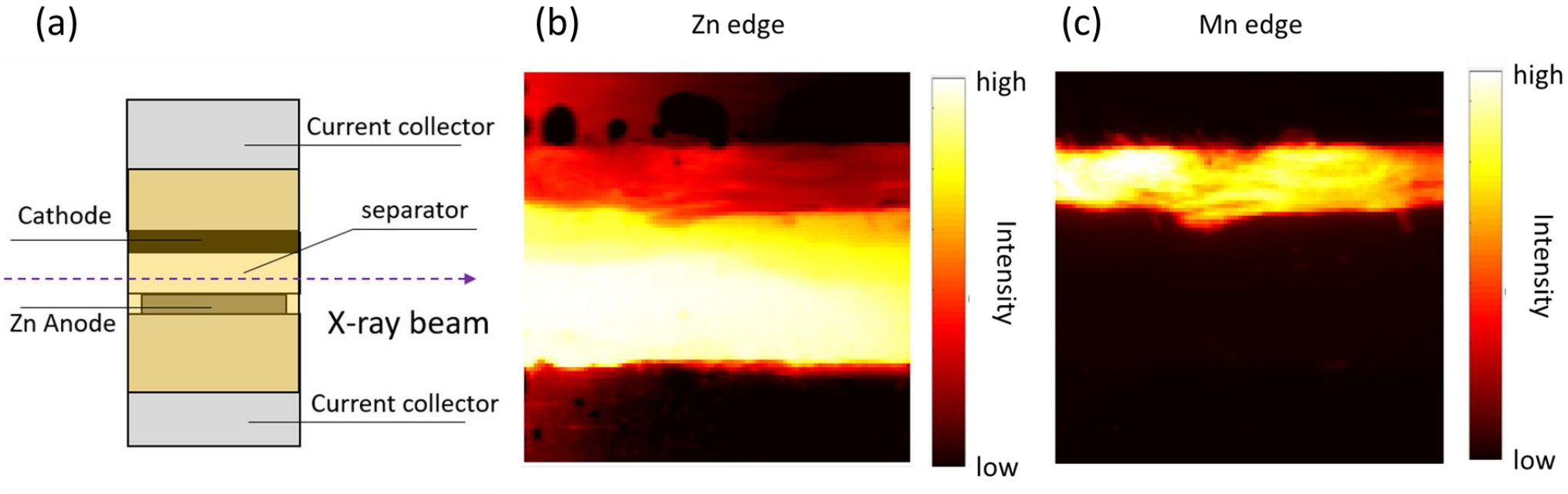

Operando cell was developed to visualize and quantify Mn^{n+} location during cycling

Operando cells exhibit comparable Galvanostatic cycling behavior with coin cells

Mn K-edge florescence maps collected repeatedly during cycling

Beamline 4-BM, X-ray Fluorescence Microprobe (XFM) at NSLS-II

D. Wu, L.M. Housel, S-J. Kim, N. Sadique, C.D. Quilty, L. Wu, R. Tappero, S.L. Nicholas, S. Ehrlich, Y. Zhu, A.C. Marschilok, E.S. Takeuchi, D.C. Bock, K.J. Takeuchi, Energy & Environmental Science (2020). DOI: 10.1039/d0ee02168g.

Operando XRF Mapping During Intermittent Discharge

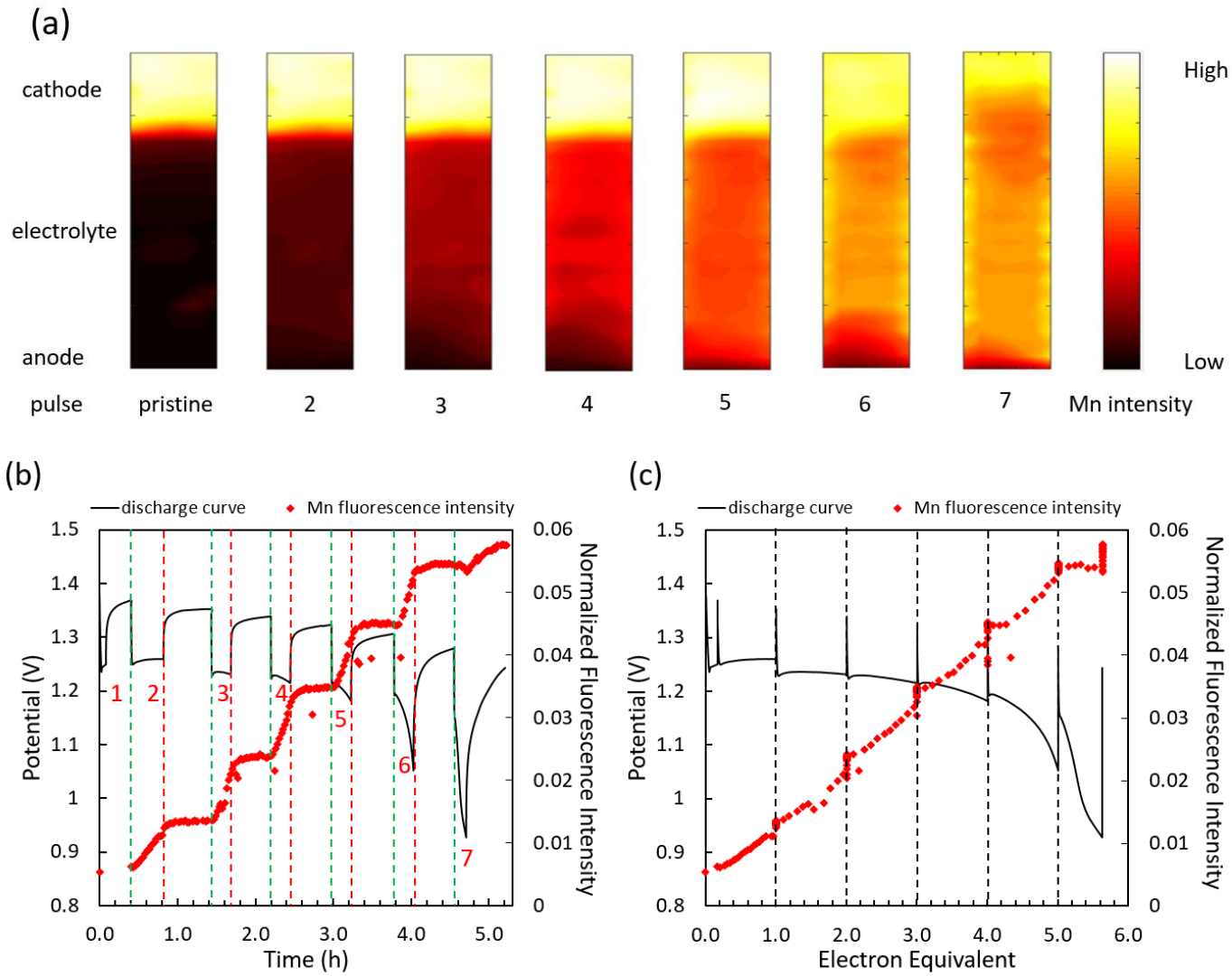

$Zn/\alpha\text{-}MnO_2$ *operando* cell discharged in 15 minute steps, each followed by an open circuit potential rest

Mn fluorescence maps, collected every 2 minutes

Increase in Mn fluorescence intensity observed in the electrolyte after each current discharge increment

Mn dissolution is an electrochemically driven process

D. Wu, L.M. Housel, S-J. Kim, N. Sadique, C.D. Quilty, L. Wu, R. Tappero, S.L. Nicholas, S. Ehrlich, Y. Zhu, A.C. Marschilok, E.S. Takeuchi, D.C. Bock, K.J. Takeuchi, Energy & Environmental Science (2020). DOI: 10.1039/d0ee02168g.

Direct Observation of Reversible Mn Dissolution-Deposition Reaction

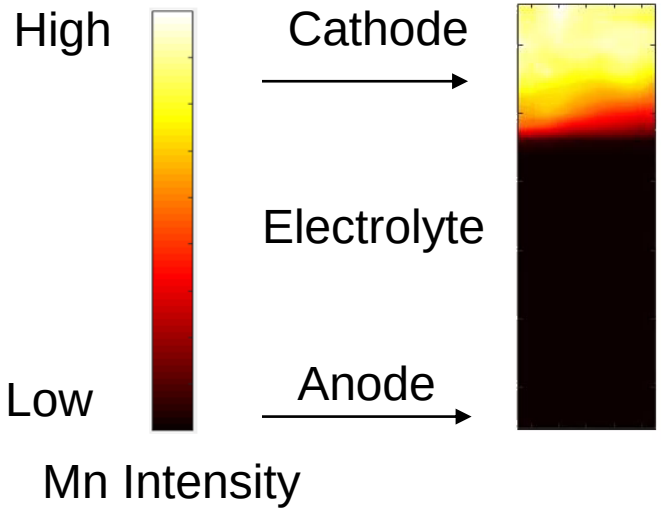

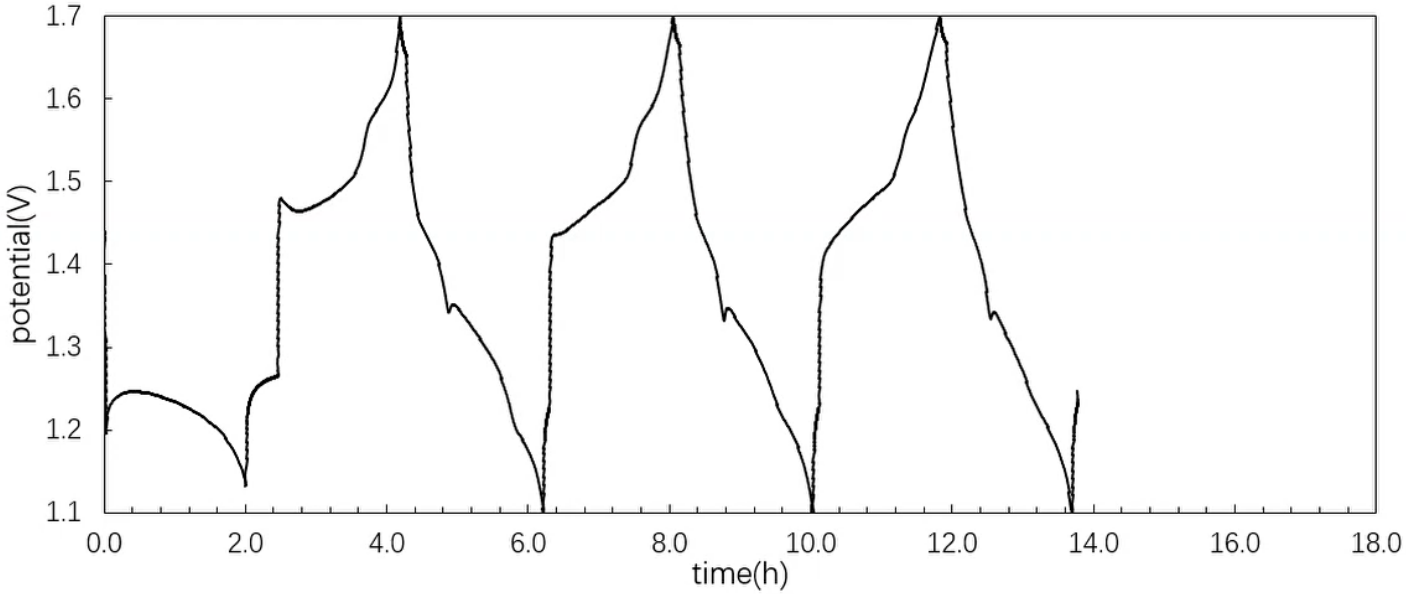

Zn/α-MnO_2 *operando* cell cycled under constant current

Mn fluorescence maps collected every ~9 minutes

Mn intensity increases in electrolyte during discharge

Mn intensity decreases in electrolyte during charge

Mn dissolution is reversible

D. Wu, L.M. Housel, S-J. Kim, N. Sadique, C.D. Quilty, L. Wu, R. Tappero, S.L. Nicholas, S. Ehrlich, Y. Zhu, A.C. Marschilok, E.S. Takeuchi, D.C. Bock, K.J. Takeuchi, Energy & Environmental Science (2020). DOI: 10.1039/d0ee02168g.

Quantification of Dissolved Mn in Cycled *Operando* Cell

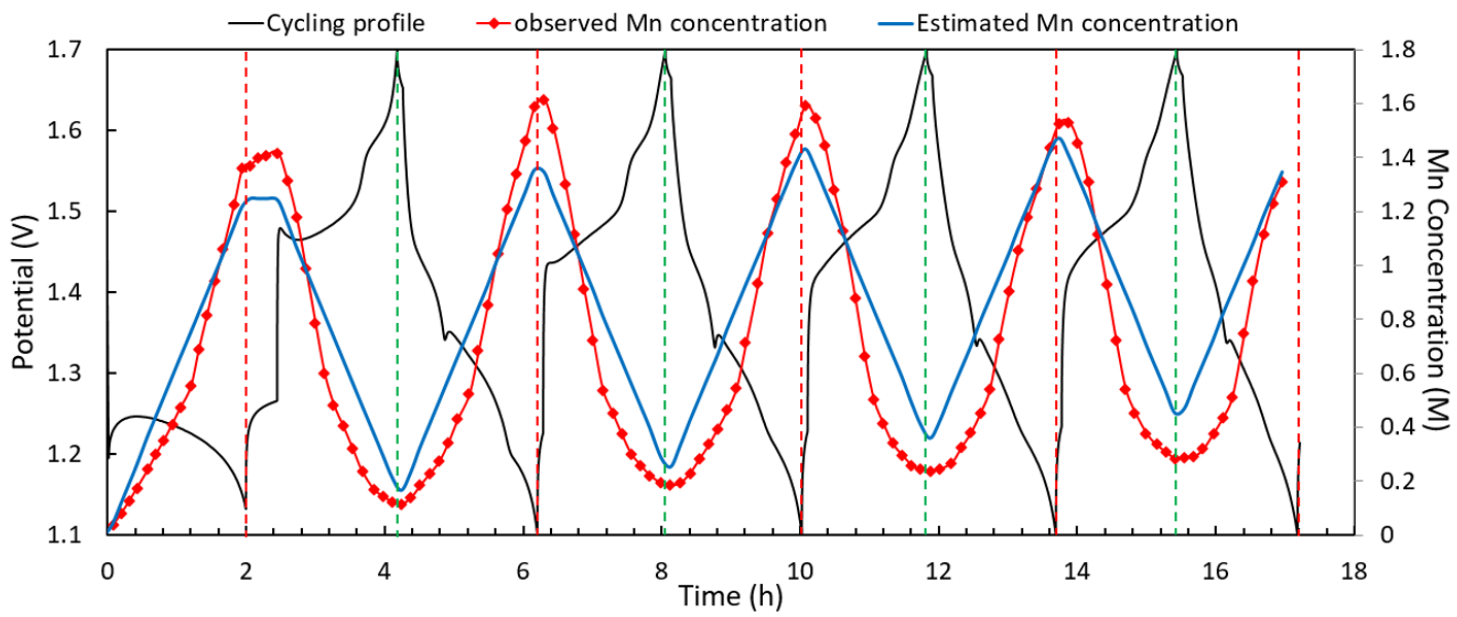

XANES spectra of dissolved species are consistent with XANES spectra of $Mn^{2+}_{(aq)}$ standard.

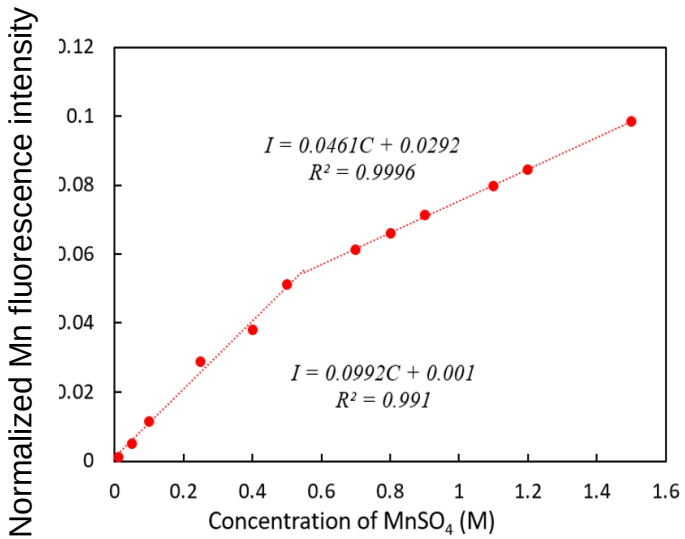

Mn Fluorescence Intensity quantified by constructing a calibration curve.

Estimated $[Mn^{n+}]$ calculated from electrochemistry assuming Dissolution-Deposition as sole Faradaic mechanism.

$$MnO_{2(s)} + 4H^+ + Zn_{(s)} \rightleftharpoons Mn^{2+}_{(aq)} + 2H_2O + Zn^{2+}$$

Measured $[Mn^{n+}]$ determined from averaging XRF maps in electrolyte region and using calibration curve.

Mn dissolution-deposition is a dominant charge storage mechanism

D. Wu, L.M. Housel, S-J. Kim, N. Sadique, C.D. Quilty, L. Wu, R. Tappero, S.L. Nicholas, S. Ehrlich, Y. Zhu, A.C. Marschilok, E.S. Takeuchi, D.C. Bock, K.J. Takeuchi, Energy & Environmental Science (2020). DOI: 10.1039/d0ee02168g.

The Dissolution-Deposition Zn/α-MnO_2 Mechanism

Discharge Mn^{2+} is dissolved into electrolyte, $Zn_4SO_4(OH)_6 \cdot 5H_2O_{(s)}$ (ZHS) precipitates on the surface

Zn +

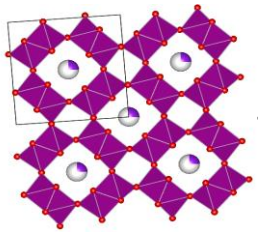

α-MnO_2

→ Mn^{2+} +

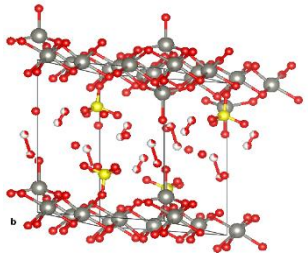

ZHS

Charge Mn^{2+} redeposits as layered $ZnMn_3O_7 \cdot 3H_2O_{(s)}$ (Chalcophanite) or (broken) tunneled MnO_2 and ZHS dissolves.

Mn^{2+} +

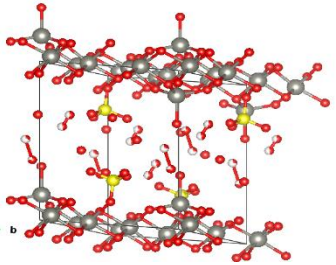

ZHS

→

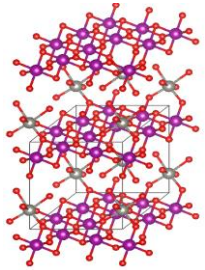

$ZnMn_3O_7 \cdot 3H_2O$

+

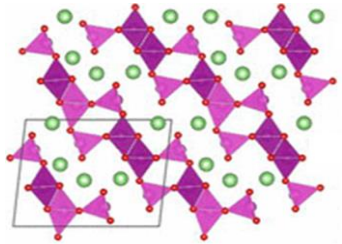

Broken Tunneled α-MnO_2

+ Zn^{2+}

Total Reaction

$$4Zn_{(s)} + ZnMn_3O_7 \cdot 3H_2O_{(s)} + MnO_{2(s)} + SO_{4(aq)}^{2-} + 12H_{(aq)}^{+} \rightleftharpoons Zn_4SO_4(OH)_6 \cdot 5H_2O_{(s)} + Zn_{(aq)}^{2+} + 4\,Mn_{(aq)}^{2+} + H_2O_{(l)}$$

D. Wu, L.M. Housel, S-J. Kim, N. Sadique, C.D. Quilty, L. Wu, R. Tappero, S.L. Nicholas, S. Ehrlich, Y. Zhu, A.C. Marschilok, E.S. Takeuchi, D.C. Bock, K.J. Takeuchi, Energy & Environmental Science (2020). DOI: 10.1039/d0ee02168g. c

Summary and Significance

First direct demonstration of Mn dissolution-deposition as the dominant charge storage mechanism for Zn/α-MnO_2 batteries achieved via *operando* XRF mapping.

Crystallographic and atomic structure and chemical state of discharge and charge products elucidated via complimentary XRD, STEM, XANES, and EXAFS.

Identification of Mn dissolution-deposition as the major mechanism provides greater understanding and builds the foundation for future innovation based on this mechanistic paradigm.

D. Wu, L.M. Housel, S-J. Kim, N. Sadique, C.D. Quilty, L. Wu, R. Tappero, S.L. Nicholas, S. Ehrlich, Y. Zhu, A.C. Marschilok, E.S. Takeuchi, D.C. Bock, K.J. Takeuchi, Energy & Environmental Science (2020). DOI: 10.1039/d0ee02168g.

Acknowledgements

Takeuchi – Marschilok Research Group- 2020

Distinguished Teaching Professor Kenneth Takeuchi

Associate Professor Amy Marschilok

Acknowledgements

Material synthesis and electrochemistry was supported by the Office of Electricity Delivery and Energy Reliability. The synchrotron studies were supported as part of the Center for Mesoscale Transport Properties, an Energy Frontier Research Center supported by the U.S. Department of Energy, Office of Science, Basic Energy Sciences, under award #DE-SC0012673.

William and Jane Knapp Chair in Energy and the Environment